energies

MDPI

Article

Hygrothermal Performance of the Hemp Concrete Building Envelope

Aguerata Kaboré , Wahid Maref * and Claudiane M. Ouellet-Plamondon

Department of Construction, École de Technologie Supérieure, Montreal, QC H3C 1K3, Canada; aguerata.kabore.1@ens.etsmtl.ca (A.K.); claudiane.ouellet-plamondon@etsmtl.ca (C.M.O.-P.)
* Correspondence: wahid.maref@etsmtl.ca

Abstract: The search for environmentally friendly and low-carbon-footprint construction materials continues progressively. Researchers are now interested in innovative materials that connect with the principles of sustainable construction, and materials such as hemp concrete prove to be promising. This article presents the results of a study that aimed to evaluate the hygrothermal performance of hemp concrete integrated into the building envelope using the hygrothermal tool WUFI Pro 6.2. The simulation model was compared and verified with existing models before its utilization for this study. The results of this verification were in good agreement, which gave us more confidence in its application for further parametric studies of building envelopes in hot climate zones. Three wall systems were simulated: (i) a wall system with hemp concrete, (ii) a compressed earth block wall, and (iii) a cement block wall. The most important variables used in the simulations were the hygrothermal properties of the materials or wall components and the incident solar radiation. The simulation results showed that hemp concrete has good thermal performance and temperature and humidity regulation capabilities of the building envelope. The interior surface temperatures of the hemp concrete walls were between 22.1 °C and 24.6 °C compared to the compressed earth block and cement block walls, where the surface temperatures were between 22.0 °C and 27 °C and between 21.2 °C and 28.7 °C, respectively, and between 23 °C and 45 °C for the exterior temperatures. These values remain the same with the increase in exterior temperatures for hemp concrete walls. In conclusion, hemp concrete could be a great alternative material for use in construction for hot climate zones.

Keywords: hygrothermal properties; hemp concrete; earth brick; cement block; biosourced; heat; CO_2 emissions; building

Citation: Kaboré, A.; Maref, W.; Ouellet-Plamondon, C.M. Hygrothermal Performance of the Hemp Concrete Building Envelope. *Energies* **2024**, *17*, 1740. https://doi.org/10.3390/en17071740

Academic Editors: Hom Bahadur Rijal, Manoj Kumar Singh and Sally Shahzad

Received: 19 February 2024
Revised: 31 March 2024
Accepted: 2 April 2024
Published: 4 April 2024

1. Introduction

The construction sector is responsible for more than 32% of total energy consumption and accounts for one third of Greenhouse Gas Emissions [1,2]. To enhance the energy efficiency of buildings, which contribute to nearly half of Greenhouse Gas Emissions, scientists prioritize the need to improve the building envelope before even considering improving the cooling and heating systems [3,4]. The determining factor in reducing a building's demand for cooling or heating energy is the quality of the design of its wall systems, roofs, windows, etc. Hence, the goal of the current research study is to focus on the building components, designed with biosourced materials, aiming to reduce their energy demand. Hemp concrete is one of those materials studied for its use in modern construction. The part of hemp used in construction is hemp stalk. This constitutes 55% of hemp straw and is the primary raw material for producing hemp concrete [5]. It has an extremely porous structure, which gives it an interesting insulating power [6,7].

Hemp concrete is a composite, porous, heterogeneous, and non-load-bearing material, generally used as insulation in a wood-frame structure [8,9]. The binders used are lime (the most commonly used), cement, pozzolan, etc. [7,10]. Hemp concrete has a dry density between 200 and 700 kg/m^3 [11–19]. It has excellent thermal inertia, excellent sound insulation, and very remarkable hygrometric regulation qualities (Moisture Buffer Value (MBV) > 2 g/m^2 % RH), demonstrating its capacity to regulate the ambient relative humidity according to the type of use [10,20–24]. In addition, hemp concretes using lime as a binder have a high water vapor permeability of the order of 10–11 to 10–10 kg/(m·s·Pa), a thermal conductivity of the order of 0.06 to 0.19 W/(m·K), and a total porosity of 72% to 85% [17,24]. The authors of a few studies obtained thermal conductivity values for this material ranging from 0.089 to 0.12 W/(m·K), and total porosities of the order of 73% to 81%, with a density between 361 and 537 k/m^3 [25–27]. The use of this material in construction contributes not only to improving the building envelope in terms of internal thermal comfort but also to reducing its energy consumption, which is currently the key element in studies on the energy efficiency of buildings. Indeed, the porosity of hemp concrete plays an essential role in the functioning of the building envelope with its ability to regulate temperature and humidity. Moreover, it favors thermal insulation by the important trapping of air [12].

Furthermore, the life cycle analysis of hemp concrete shows that it can store between 14 kg CO_{2eq} and 35 kg CO_{2eq} per square meter of the wall over 100 years [16,22,28]. A wood-frame building insulated with hemp concrete contributes to a reduction in CO_2 of about 71%, with 41% for hemp concrete and 30% for wood-frame buildings compared to a traditional concrete block wall [28]. In terms of gray energy, it takes 6 times more energy to produce glass wool than hemp wool, and the gray energy of solid brick is 16 times higher than that of hemp concrete [7]. In terms of value, the gray energy of hemp wool is 35 kWh/m^3, while that of glass wool is 250 kWh/m^3 [29], that of hemp concrete is 90 kWh/m^3, and that for solid brick is 1443 kWh/m^3 [28]. The advantages of using hemp concrete in construction are related to its low gray energy, good thermal resistance, and low thermal conductivity, which gives hemp concrete good insulating properties. Additionally, it is a natural, renewable, recyclable, biodegradable, and CO_2 fixing material [30–32].

With such advantages, current state-of-the-art technologies used for concrete production should also be used to produce hemp concretes to study their influence on the properties of hemp concrete. These technologies have been employed to study the mechanical performance of cement concrete, such as 3D printing [33–36]. These works highlight the potential of the 3D printing of concrete. Other manufacturing methods can be implemented to improve the durability of hemp concrete, such as the use of natural pozzolan and microsilica as partial substitutes for lime in hemp concrete mixes [10,37]. A study presented an optimization model to determine the optimal mixture proportions for different types of eco-friendly concrete, using the Grey Wolf optimizer and a backpropagation neural network [38]. These works demonstrated the efficiency of the model in calculating optimal mixture proportions and highlighted the performance of eco-friendly concrete under specific parameters. This type of model could be used to optimize the proportions of raw materials to produce hemp concrete to study the influence of optimizing the composition of hemp concrete on its hygrothermal performance. In terms of thermal performance, a study demonstrated the effectiveness and cost-effectiveness of the HEAT system for the thermal monitoring of building envelopes [39]. According to the author, it is a temperature-based method that offers a cost-effective, scalable, and simplified approach to estimating thermal parameters in building envelopes. This method could also be a valuable tool for the effective thermal monitoring of hemp concrete buildings. Additionally, the use of new data acquisition systems would be necessary to obtain the thermal parameters of hemp concrete building envelopes [40].

The hygrothermal benefits of hemp concrete in cold climates, and its significant potential to reduce winter heating needs, were evaluated by Bennai et al. [41]. This research highlighted the effectiveness of hemp concrete as insulation in timber-frame structures, emphasizing its role in lowering energy consumption and its compliance with energy efficiency and environmental standards. Analyses under static conditions and during typical summer and winter days have considered hemp concrete as a promising material [42], and these results are supported by other recent studies [27,41–45], acknowledging its revolutionary impact in the construction sector. This material therefore represents a solution for the renovation of old buildings as well as for new constructions. Despite its advantages, the use of hemp concrete in construction in some countries is not well known, due to regulations put in place against the use of hemp. However, in countries with very hot climates, the use of appropriate construction materials has become crucial. Thus, a combination of plant fibers in the design of clay bricks and adobe bricks can contribute to improving their thermal performance, as well as their resistance to different weather conditions.

Hemp concrete is a well-studied but underutilized material in construction. It faces acceptance challenges due to the industry's conservative tradition, infrastructure constraints, and the need to train building professionals on the use of this non-load-bearing material in modern construction [46]. Additionally, the lack of specific standards and regulations limits its large-scale use. Studies on hemp concrete have primarily been conducted in Europe. For its application in hot regions, evaluating the building envelope designed with this material through numerical and experimental simulation could provide an in-depth analysis of thermal and moisture performance. This approach allows for adapting and enhancing hemp concrete to meet the required performance in specific climates, thus facilitating its extensive and sustainable use in these environments [47]. By combining in-depth knowledge of hemp concrete characteristics with the results obtained through numerical simulations on its hygrothermal performance, it is possible to optimize its use in hot climate zones, promoting the broader adoption of this durable and eco-friendly material. They can thus serve as perfect insulation for mitigating heat transfer through the building's envelope in hot climate zones where the external temperature can reach 45 °C. This is what motivated the implementation of this research work through numerical simulations.

The main objective of this study is to assess the hygrothermal performance of hemp concrete for its applications in building envelopes located in hot climates. The data on hemp concrete obtained by Samri [16] in Lyon, France, are used in the WUFI Pro 6.2 simulation tool, allowing the comparison of its thermal performance with those of cement blocks and compressed earth bricks. The goal is to analyze the heat and moisture transfer through these materials, considered crucial for the performance of the building envelope. Figures 1 and 2 illustrate the evolution of the exterior temperature on a monthly basis. Burkina Faso, with its tropical climate and temperatures sometimes reaching 45 °C (Figure 2), especially in Dori City in the north of the country, illustrates the importance of this study and makes it more interesting research work. Most temperatures in this city vary throughout the year between 24 °C and 45 °C. The persistent high temperatures throughout the year underscore the constant need for cooling buildings, hence the choice of climatic data from this city for numerical simulations with WUFI Pro 6.2 software (by Hartwig M. Künzel, Fraunhofer Institute for Building Physics (IBP), Holzkirchen, Germany). The integration of ecological materials, such as hemp concrete, could not only reduce the energy consumption needed for cooling buildings in hot climate zones but also ensure better interior thermal comfort without resorting to air conditioning. However, it is necessary to consider hot and humid climate areas to properly assess the hygrothermal performance of the material.

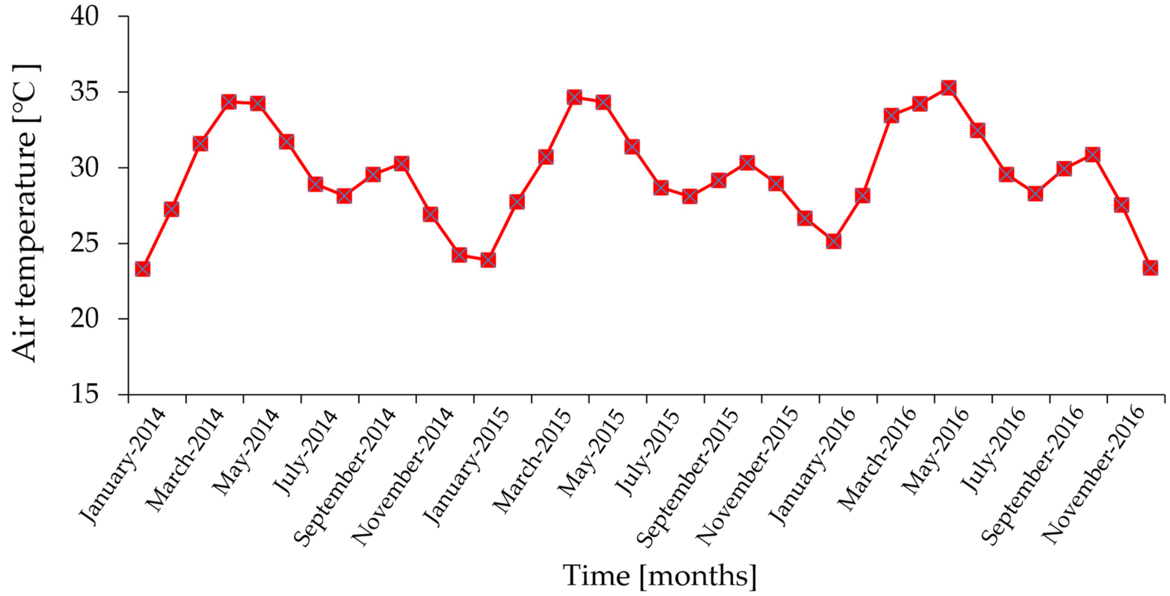

Figure 1. Overview of exterior temperature variation (monthly average) for three consecutive years in Dori (2014–2016) obtained by the National Meteorological Agency in Ouagadougou.

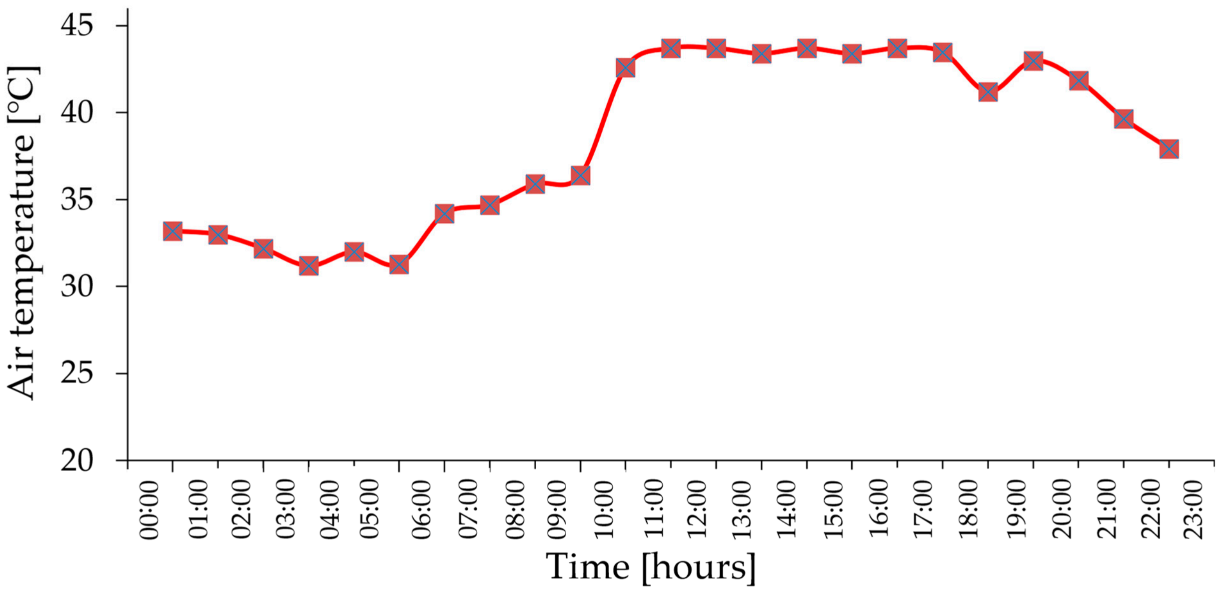

Figure 2. Temperature variation of the city of Dori for a typical day in May 2016 (3 May 2016) obtained by the National Meteorological Agency in Ouagadougou.

2. Numerical Simulations

The numerical simulation involved studying three cases of wall assemblies (i.e., building envelopes). The first case was composed of cement blocks, the second case of compressed earth bricks, and the third of hemp concrete. To increase the temperature of the exterior surface of each envelope, an amount (or fraction) of incident solar radiation of 1% to 20% was applied to their exterior surfaces. The coupled energy and mass transfer equations established by Künzel [29] were used for the numerical simulation, utilizing WUFI Pro 6.2 software. These equations are represented by (1) and (2):

✓ Energy conservation balance

$$\frac{\partial H}{\partial T} \cdot \frac{\partial T}{\partial t} = \nabla \cdot (\lambda \nabla T) + L_v \nabla \cdot (\delta_P \cdot \nabla (H_R P_{sat})) \quad (1)$$

✓ Mass conservation balance

$$\frac{\partial w}{\partial H_R} \cdot \frac{\partial H_R}{\partial t} = \nabla \cdot \left(D_\varphi \nabla H_R + \delta_P \nabla \cdot (H_R P_{sat}) \right) \quad (2)$$

where $\frac{\partial H}{\partial T} \cdot \frac{\partial T}{\partial t}$ is the thermal inertia, $\nabla \cdot (\lambda \nabla T)$ is the thermal conductivity, $L_v \nabla \cdot (\delta_P \cdot \nabla (H_R P_{sat}))$ is the liquid and vapor convection, $\frac{\partial w}{\partial H_R} \cdot \frac{\partial H_R}{\partial t}$ is the water inertia (humidity), $\nabla \cdot \left(D_\varphi \nabla H_R \right)$ is the liquid diffusion, and $\delta_P \nabla^2 \cdot (H_R P_{sat})$ is vapor diffusion. H is the enthalpy of volume in J/m^3, T is the temperature in °C, L_v is the latent heat of the phase change of water in J/kg, δ_P is the water vapor permeability of the material in kg/m·s·Pa, H_R is the relative humidity in %, P_{sat} is the saturation vapor pressure in Pa, w is the water content in kg/kg, D_φ is the vapor phase diffusion coefficient in m^2/s, ∇ is the gradient, and ∂ is the partial derivative. Before starting the hygrothermal simulation with the data of our study, verification was carried out and is presented in Section 2.1.

2.1. Model Verification: Materials and Methods

2.1.1. Validation of WUFI Pro 6.2 Models

WUFI Pro 6.2 is a well-known hygrothermal tool that has already been validated with several physical phenomena. For this research study, for the validation of the software, research data from Dhakal [30] and Lamalle [48] were used. The same hypotheses were applied in WUFI Pro 6.2 in order to compare the results with those obtained with WUFI Pro 5.1 by Dhakal [30] and Lamalle [48]. These two works were chosen because they have a complete set of data necessary for feeding the hygrothermal simulation model. Therefore, the hypotheses and boundary conditions used by the two authors are listed below so that the simulation can be performed. Thereafter, we begin our case study and parametric study with confidence in the WUFI Pro 6.2 models.

2.1.2. Wall Assembly Configuration for Validation

- For the City of Toronto defined by Dhakal [30]

The sheathing membrane "TYPAR®" is a housewrap used in this study. It has two functions: Weather or Water Resistive Barrier (WRB) and air barrier. It keeps the water and the air out of the building envelope. This material does not exist in the WUFI Pro 6.2 material database directory. It is replaced by an air barrier (3M™ vapor-permeable air barrier 3015 (3M Company, Saint Paul, MN 55144, USA)), which has almost identical hygrothermal properties. Figure 3 presents the two simulation walls performed by Dhakal [30] in his work. These two wall assemblies are used for simulation with WUFI Pro 6.2.

The input data for the hemp concrete material in WUFI Pro 6.2 were those of Dhakal [30]. By definition, the presence of a ventilated wall cavity or an air gap in wall 2 acts as a capillary break. It facilitates the drying of any water vapor that can pass through the outer wall, i.e., passing the first line of defense for the building envelope which is the exterior cladding. Table 1 shows the input data of the hemp concrete used in WUFI Pro 6.2.

The other materials making up the wall were selected from the directory of the WUFI Pro 6.2 material database. These materials already exist in the software.

- For the City of Liège defined by Lamalle [48]

All wall material data used by Lamalle were selected in WUFI Pro 5.1 except for the wood concrete data, which were entered manually. The same data were used in WUFI Pro 6.2 for verification of the results to determine the sensitivity of the version. Figure 4 illustrates the configuration of the wall established by Lamalle [48], and Table 2 presents the input data for this work.

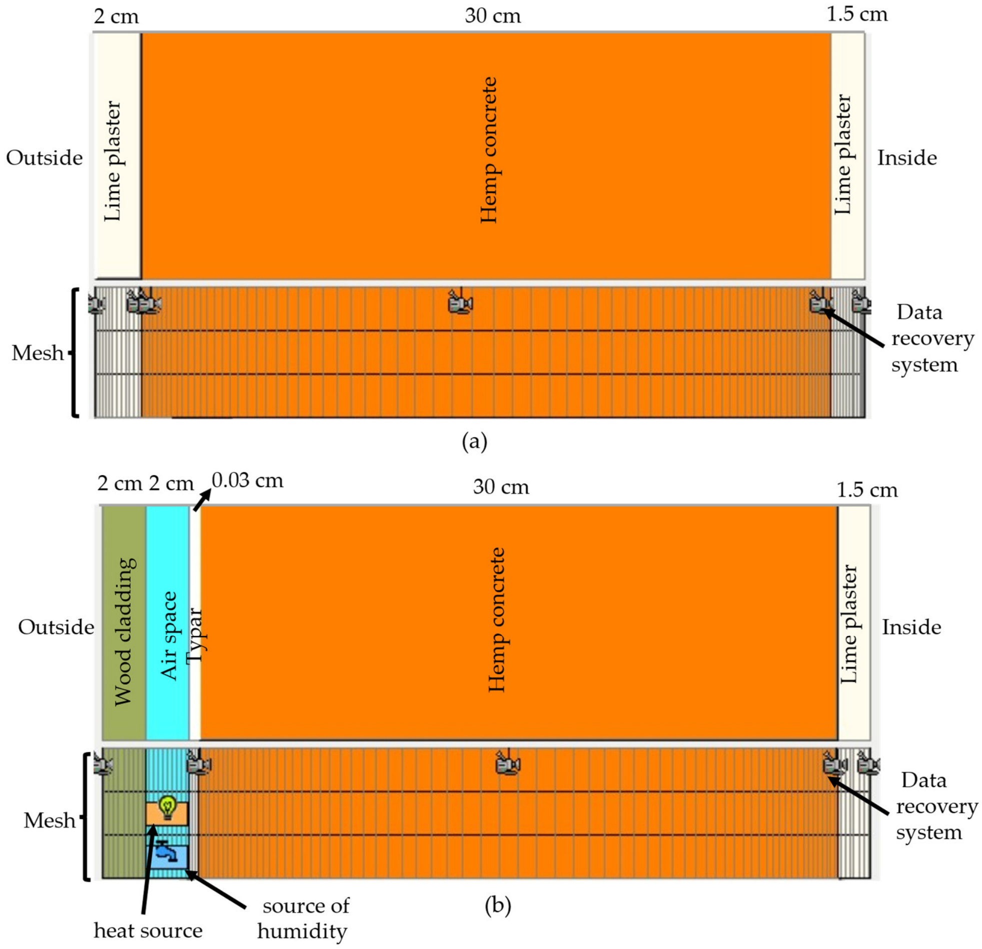

Figure 3. Wall assembly: (**a**) wall 1 and (**b**) wall 2 for the verification of WUFI Pro 6.2 with Dhakal material data [30].

Table 1. Input data for hemp concrete, data obtained from Dhakal's work [30].

Hygrothermal Property	Values
Dry density [kg/m^3]	388
The porosity of the material [-]	0.66
Specific heat in dry condition [J/kg K]	1560
Thermal conductivity dry state [W/m K]	0.1
Dry vapor diffusion resistance factor	4.85
Moisture-dependent thermal conductivity supplement [% M, %]	3.34
Maximum water content [kg/m^3]	655
Open water saturation [kg/m^3]	424
Moisture content at 80% [kg/m^3]	29
Liquid absorption coefficient	0.074
Humidity type of construction [kg/m^3]	286

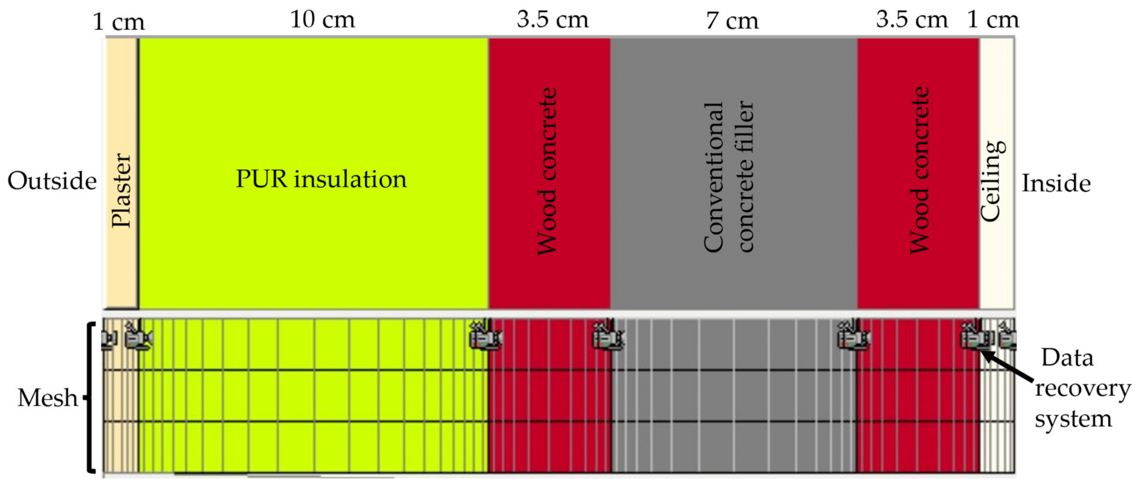

Figure 4. Wall assembly for validation of WUFI Pro 6.2 with Lamalle materials data [48].

Table 2. Materials' input data.

Layer Name	Material in the Database	Density [kg/m³]	Porosity [-]	Thermal Conductivity [W/m·K]	Resistance to Diffusion [-]
Plaster	Exterior mineral plaster	1900	0.24	0.8	25
Polyurethane Rigid Foam (PUR) insulation	PUR	40	0.95	0.03	50
Wood concrete	Concrete block of expanded clay	800	0.67	0.1	4
Conventional concrete filler	Concrete E/C = 0.5	2300	0.18	1.6	180
Ceiling	Interior ceiling (plaster)	850	0.65	0.2	8.3
Wood fiber panel	Wood fiber panel	300	0.8	0.05	12.5
Cellulose insulation	Cellulose fiber	50	0.95	0.034	1.8
Foamed concrete filler	Cellulose concrete	500	0.77	0.12	8

2.1.3. Simulation Assumptions

To start using WUFI Pro 6.2 software, the assumptions used are listed in Table 3.

Table 3. Assumptions for verification with data from Dhakal, 2017 [30] and Lamalle, 2016 [48].

Number	Assumptions
1	Samples—isotropic, homogeneous, and without volumetric variation
2	No chemical reaction between water in all 3 phases
3	No energy dissipation during flow
4	Except for weather, no parameter depends on the time of day
5	No univalent relationship between water content and relative humidity
6	No air infiltration (airtight wall)
7	No relevance of temperature in moisture sorption
8	No advection
9	Perfect contact between materials

2.1.4. Boundary Conditions for Simulation

For the exterior climate, the weather file of the city of Toronto, as presented in the files of WUFI Pro 6.2, was used for the verification simulation. The data climate files of Liege in Belgium produced by Lamalle [48] were introduced in WUFI Pro 6.2 to be able to perform the simulation. For the interior climate, the sine curve giving the variation in the interior temperature used by Dhakal [30], and the conditions following the EN 15 026 standard [49] by Lamalle [48], were implemented. The boundary conditions used by each author were also applied in WUFI Pro 6.2. These boundary conditions are listed in Table 4.

Table 4. Boundary conditions for simulation.

Number	Boundary Conditions
1	Interior environment: 21 °C ± 1 °C, RH 50 ± 10% (sinusoidal curve for Dhakal and EN 15 026 for Lamalle)
2	Initial state: 20 °C and 80% RH (constant in the component) for both authors and for WUFI Pro 6.2
3	Southeast orientation [30] and west orientation [48] to maximize the combination of sun exposure and rain expectation; vertical surfaces [R1 = 0, R2 = 0.07 m/s; short building—height up to 10 m], with R1 and R2 as the driving rain coefficients that depend strongly on the position of the external façade
4	Short-wave absorptivity (shiny limestone and untreated spruce) = 0.4
5	Rainwater absorption factor α_r = 0.7
6	No surface coating
7	ACH-8 for the air layer (ventilated) for assembly 2 [30], and for the rest of the assemblies, there is no air layer, where ACH is the Air Change per Hour
8	Cloud index or average cloud index: 2.64 for Dhakal and 0.64 for Lamalle (analyzed from weather files)
9	Simulation period is 3 years each: from 1 October 2015 to 1 October 2018 for Dhakal, and from 1 October 2016 to 1 October 2019 for Lamalle
10	The others, not mentioned, are taken by default as in the works of Dhakal and Lamalle
11	Heat transfer coefficients (interior h_i and exterior h_e): program default (constant coefficient), h_i = 8.0 W/m^{2}K, h_e = 17.0 W/m^{2}K

The boundary conditions were entered into WUFI Pro 6.2 manually or selected directly from the software database as indicated by the two authors. Windows were specially designed to introduce the boundary conditions, wall design, and assumptions into the software.

2.1.5. Conformity Check: WUFI Pro 6.2 Results Compared to Dhakal and Lamalle

- Conformity of WUFI Pro 6.2 results with those of Dhakal

When starting the calculations with the simulation tool WUFI Pro, an animation is proposed by the software to visualize the temperature curves, relative humidity, and water content in the wall. The curves obtained after simulations were compared with those of Dhakal, obtained with WUFI Pro 5.1. The simulation results of walls 1 and 2 for the City of Toronto covered the period from 1 October 2015 to 1 October 2018. Table 5 presents a summary of the heat and moisture flow from the wall to interior and exterior environments. It also shows the total moisture content at the start and end of the simulation, including the maximum and minimum moisture content levels.

Table 5. Flow integral versus time and total moisture content (wall 1).

	Unit	WUFI Pro 6.2	Dhakal [30]
Heat flow, left side	[MJ/m^2]	−489.01	−489.01
Heat flow, right side	[MJ/m^2]	−487.69	−487.69
Moisture flow, left side	[kg/m^2]	0.84	0.84
Moisture flow, right side	[kg/m^2]	2.62	2.62
Total water content (start of the simulation)	[kg/m^2]	9.75	9.75
Total water content (end of the simulation)	[kg/m^2]	7.98	7.98
Minimum value	[kg/m^2]	7.78	7.78
Maximum value	[kg/m^2]	17.57	17.57

The benefit of checking the models used for the simulation is that it gives you confidence in which model to use for further work and what results will be obtained. Figure 5 shows the total water content curves for walls 1 and 2. Figure 6 shows the hemp concrete water content for wall 1 obtained from Dhakal and the WUFI Pro 6.2 simulations, for the period from 1 October 2015 to 1 October 2018.

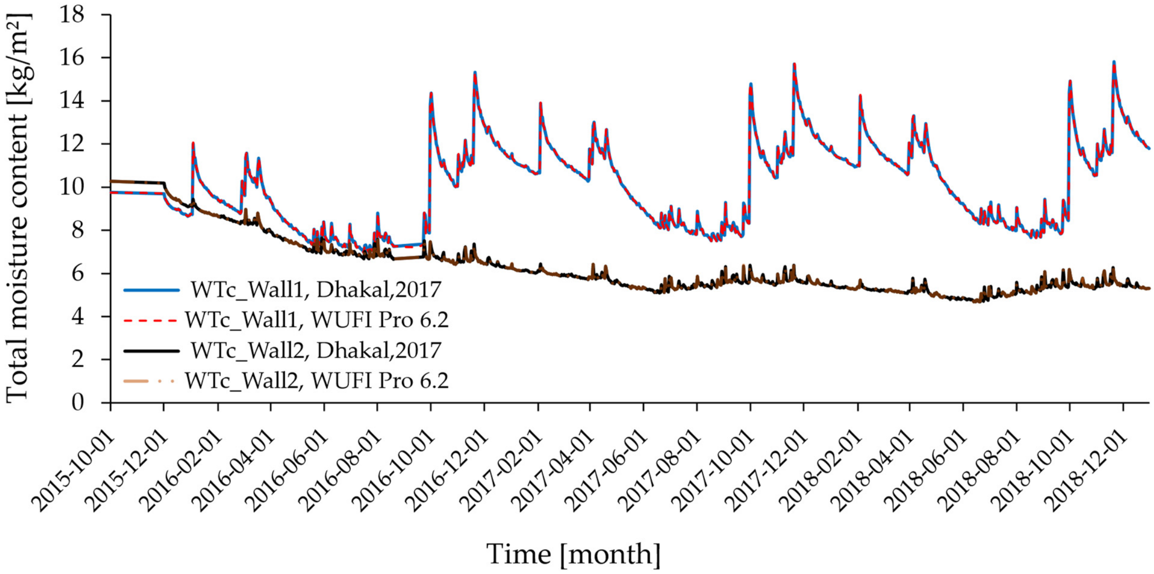

Figure 5. Total moisture content (WTc) of walls 1 and 2 for Dhakal [30] and WUFI Pro 6.2.

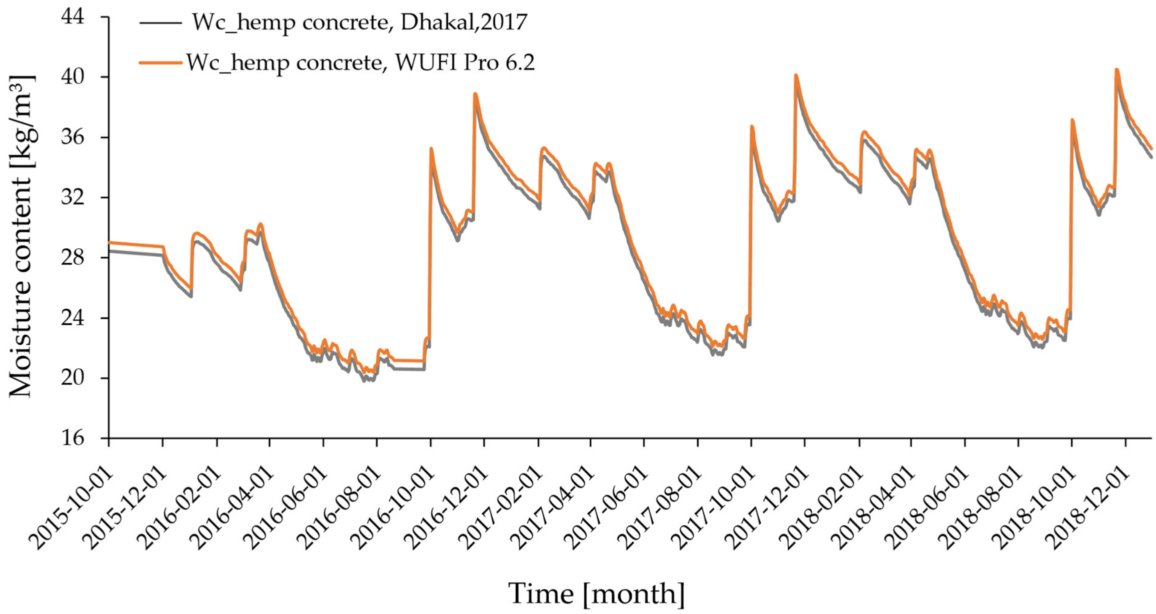

Figure 6. Moisture content (Wc) of hemp concrete in wall 1 for Dhakal [30] and WUFI Pro 6.2.

The results obtained by WUFI Pro 6.2 are in good agreement with those of Dhakal [30] (Figure 5). However, for the hemp concrete water content curve (Figure 6), a slight difference between the two results obtained was observed, with a maximum difference of 0.01 kg/m^3. Before concluding the validation of WUFI Pro 6.2, a last simulation with the data from the work of Lamalle was performed.

- Conformity of WUFI Pro 6.2 results with those of Lamalle [48]

Figures 7 and 8 present the simulation results for the period from 1 October 2016 to 1 October 2019 and those obtained by Lamalle. These figures allow the observation of the distribution of water contents in all the walls. The results obtained by WUFI Pro 6.2 are in good agreement with those obtained by Lamalle.

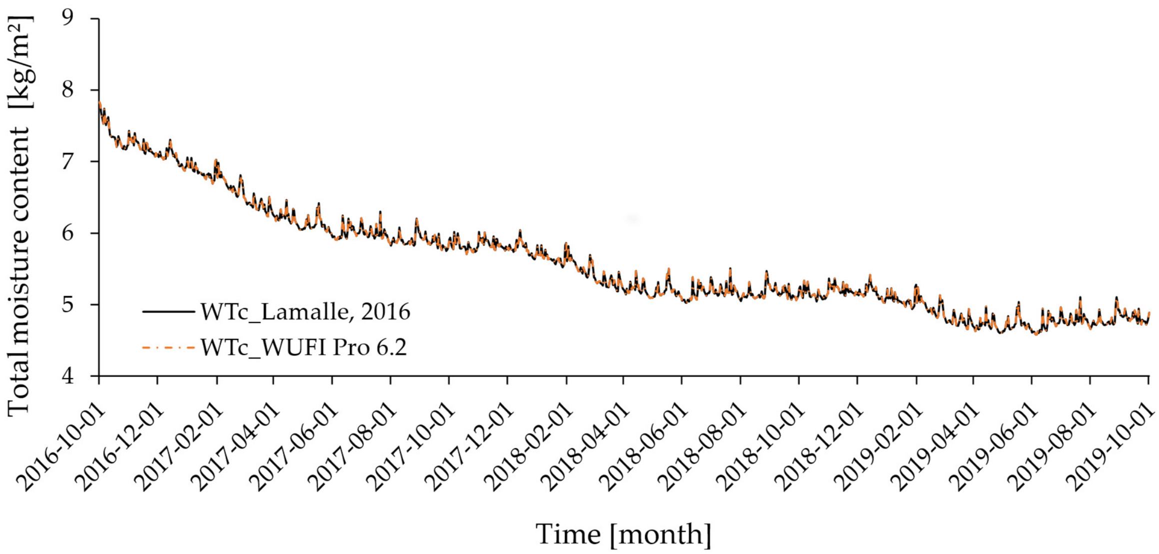

Figure 7. Total wall moisture content (WTc), results from Lamalle [48] and WUFI Pro 6.2.

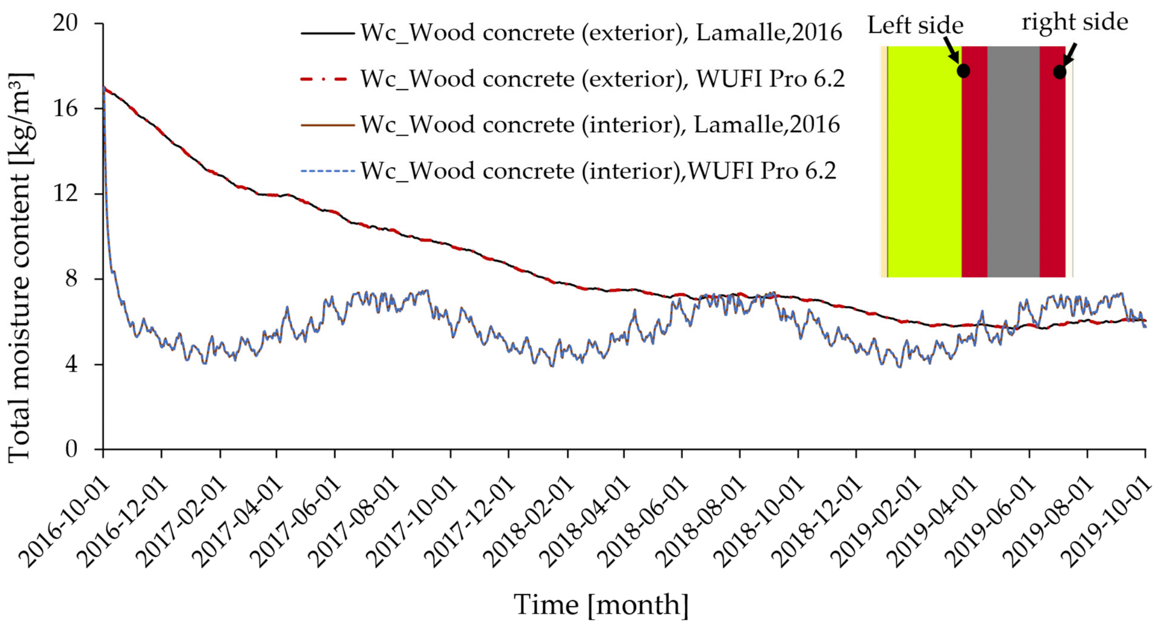

Figure 8. Moisture content (Wc) of wood concrete, left side (exterior) and right side (interior); results from Lamalle [48] and WUFI Pro 6.2.

The studies by Dhakal in 2017 and Lamalle in 2016 were conducted on the hygrothermal performance of hemp concrete and wood concrete, respectively. These studies found that hemp concrete and wood concrete are environmentally friendly materials that are suitable for construction due to their performance in regulating humidity and interior temperature. Analyses of the results of these studies are available in the work of Dhakal et al. [30] and Lamalle [48]. For the software validation, we can confirm the authenticity of the results obtained by WUFI Pro 6.2 and WUFI Pro 5.1 (the version used by Dhakal and Lamalle). After the verification of WUFI Pro 6.2, we could establish the assumptions, boundary conditions, and hygrothermal properties of the materials that were used in the current study. Thus, regardless of the version of WUFI Pro used to simulate the data, the obtained results would be the same. The rest of this work consists of varying the material variables and introducing the weather data of the city to be studied to start the simulation.

2.2. Case of Our Study: Materials and Methods

After verifying the results with the model that was used for the rest of this work, we could continue with the study of the performance of hemp concrete with full confidence. The present study involved assessing the thermal performance of hemp concrete in three cases of the building envelope, using weather data from Dori City in Burkina Faso. The data on hemp concrete from the study carried out in the city of Lyon in France by Samri [16] were used. This study involved conducting simulations on the coupled heat and moisture transfer for various types of wall assemblies. This simulation analyzed the ability of hemp concrete to manage heat compared to cement blocks and compressed earth brick. Figure 9 shows the structural configuration of the wall system.

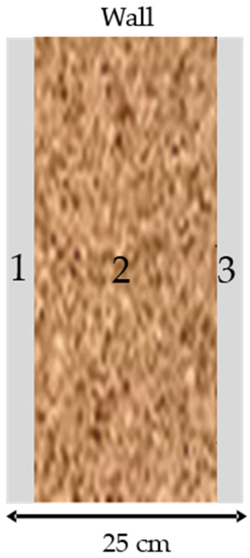

Figure 9. Wall components: (1) cement plaster exterior; (2) concrete hemp (HLC2), cement block or compressed earth brick, and (3) cement or lime plaster interior.

A cement block wall, a compressed earth brick wall, and a hemp concrete wall were simulated. On the exterior surface of these walls, five scenarios were established in each case. For the first two scenarios, an increase in the incident solar radiation fractions by 1% and 5% was applied to observe the amount of heat able to pass through each wall to the interior (Figures 10 and 11). For the next three scenarios, increases of 10%, 15%, and 20% were applied with the aim of increasing the heat reaching the exterior surfaces of the walls (Figure 11). By definition, the fraction of incident solar radiation refers to the percentage of the total solar radiation that reaches and is absorbed by a surface or material. The goal of increasing heat on the exterior surfaces of the walls is to observe their capacity to store heat on their exterior surface and its influence on the interior temperature of the walls. To conduct the numerical simulation, the data of hemp concrete were inputted into the database of the WUFI Pro 6.2 software. Table 6 shows the composition of each wall component, including thicknesses, and Table 7 shows the properties of each material. Given that the weather data came from the city of Dori, the typical thickness of a wall assembly in Burkina Faso is about a maximum of 30 cm including the exterior and interior plaster. All cases conformed to a typical construction in Burkina Faso.

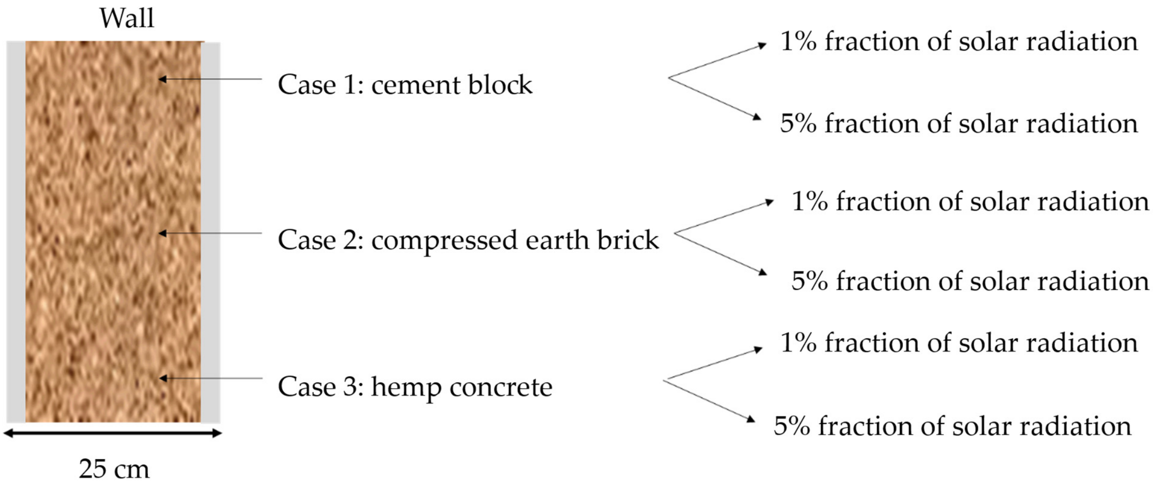

Figure 10. Building envelope components for this study.

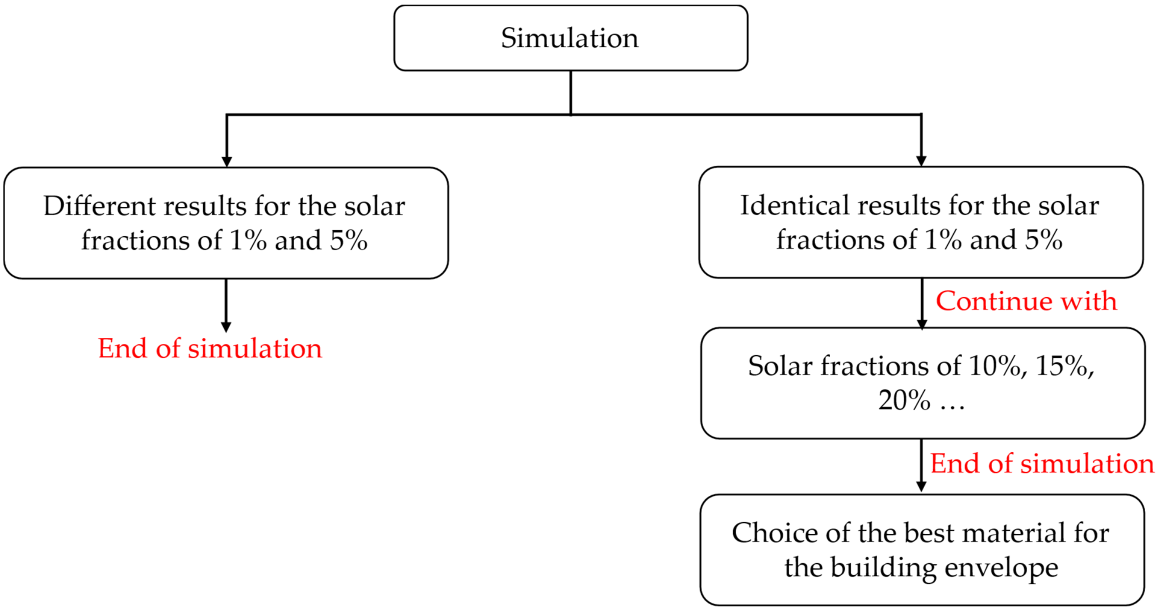

Figure 11. Stepwise approach simulations for the city.

Table 6. Composition of each building envelope studied in WUFI Pro 6.2.

Case 1: Cement Block Wall	Case 2: Compressed Earth Brick Wall	Case 3: Hemp Concrete Wall
Plaster: 1 cm Cement block: 23 cm Plaster: 1 cm	Plaster: 1 cm Compressed earth brick: 23 cm Plaster: 1 cm	Plaster: 1 cm HLC2 hemp concrete: 23 cm Plaster: 1 cm

Table 7. Properties of envelope components.

Layer Name	Materials in the Database	Density [kg/m^3]	Porosity [-]	Thermal Conductivity [W/mK]	Specific Heat [J/kgK]	Diffusion Resistance [-]
Roughcast	Cement plaster	2000	0.3	1.2	850	25
Cement block	Concrete W/C = 0.5	2300	0.18	1.6	850	180
HLC2 hemp concrete	HLC2 hemp concrete	317	0.79	0.085	1000	3.6
Compressed earth brick	Compressed earth brick	2100	0.24	0.8	1732	10
Painting	Lime plaster	1600	0.3	0.7	850	7
Air blade	20 mm air blade	1.3	0.999	0.071	1000	0.73

2.2.1. Boundary Conditions and Assumptions

The boundary conditions were set according to the interior and exterior climates of the city of Dori. A weather sheet was generated from climate data obtained by the National Meteorological Agency in Ouagadougou for the city of Dori and was used for the simulation. These data contain climatic data taken every 15 min. They were analyzed and post-processed to obtain data in hours that can be used by WUFI Pro 6.2. The simulation was carried out over a period of 3 years, from 1 January 2014 to 1 January 2017. The load due to rain (the amount of rain that reaches the wall) was determined according to the ASHRAE 160 standard, 2009 [50], based on the Wind-Driven Rain data in the weather file. The boundary conditions were established as illustrated by Figure 12.

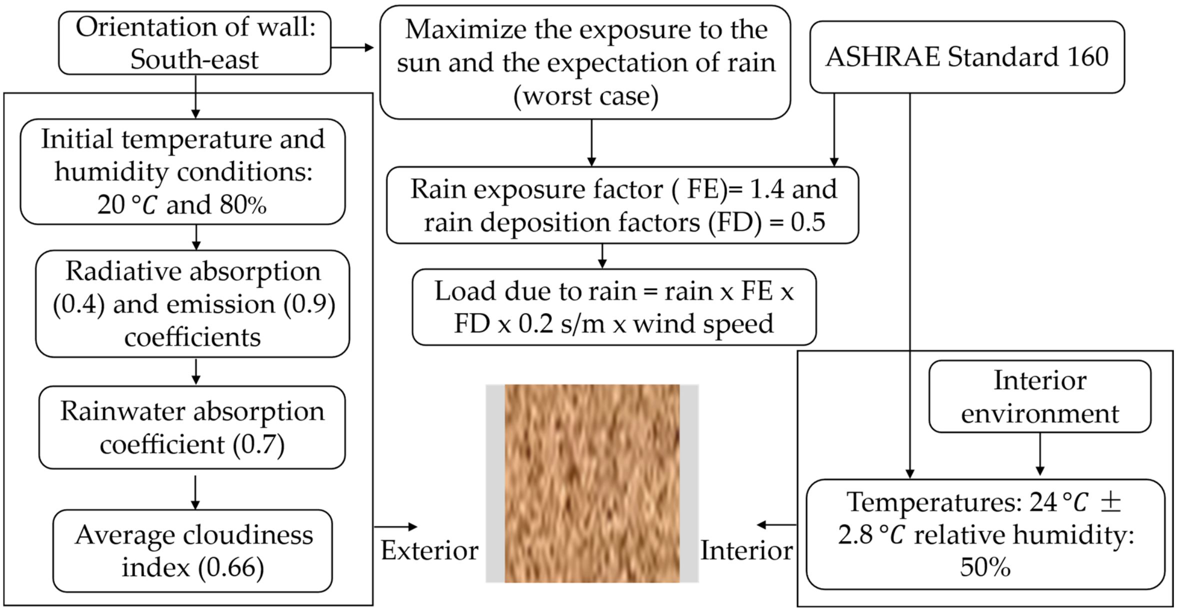

Figure 12. Boundary conditions.

2.2.2. Assumptions Made for the Study

1. No water infiltration in the wall, except due to Wind-Driven Rain (WDR),
2. The simulation considers that the airtightness is well achieved.

3. Results

The simulation was conducted over three years, utilizing climate data available (from 1 January 2014 to 1 January 2017). Figures 13 and 14 illustrate the variation in temperature and humidity over these consecutive years. In Dori, a city known for its high temperatures, our study focused on three key aspects of thermal management. First, we examined the ability of the exterior surfaces of the walls to store heat. Second, we evaluated the ability of the walls to regulate interior temperature. Lastly, we investigated the variations in interior temperature by applying a surplus incident solar radiation fraction of 20%. However, the variations in humidity through the interior walls were evaluated before selecting the results to be presented in this article. Humidity data were not included in this article, because exterior humidity is mostly below 80%, with almost no rain for more than 10 months. For future studies, it is therefore important to use climate data that includes both high temperatures and high humidity, which can reach 100% over several months. This will allow for a more precise evaluation of hygrothermal performance in hot and humid zones.

The data presented in Table 8 illustrate the variation in temperature on the exterior surface, the middle, and the interior surface for each simulation case. The accumulation of heat on the exterior surface of the hemp concrete wall was higher in summer than those of the cement block wall and the compressed earth brick wall. In winter, the temperature dropped to 9 °C, a value lower than those of the other walls. Therefore, the hemp concrete accumulated more heat on its exterior surface during the warm season. With the interior setpoint fixed at 24 °C, the interior temperature of the hemp concrete envelope decreased by 2 °C in winter and increased by 0.5 °C in summer. For the cement block wall, a temperature decrease of 4 °C was observed in winter and an increase of 5 °C was observed in summer, while the compressed earth brick wall experienced a decrease of 3 °C in winter and an increase of 3 °C in summer. Applying an incident solar radiation fraction of 1% and 5% resulted in similar interior temperatures. In conclusion, increasing the overall solar radiation by 5% had no influence on the interior temperature of each wall.

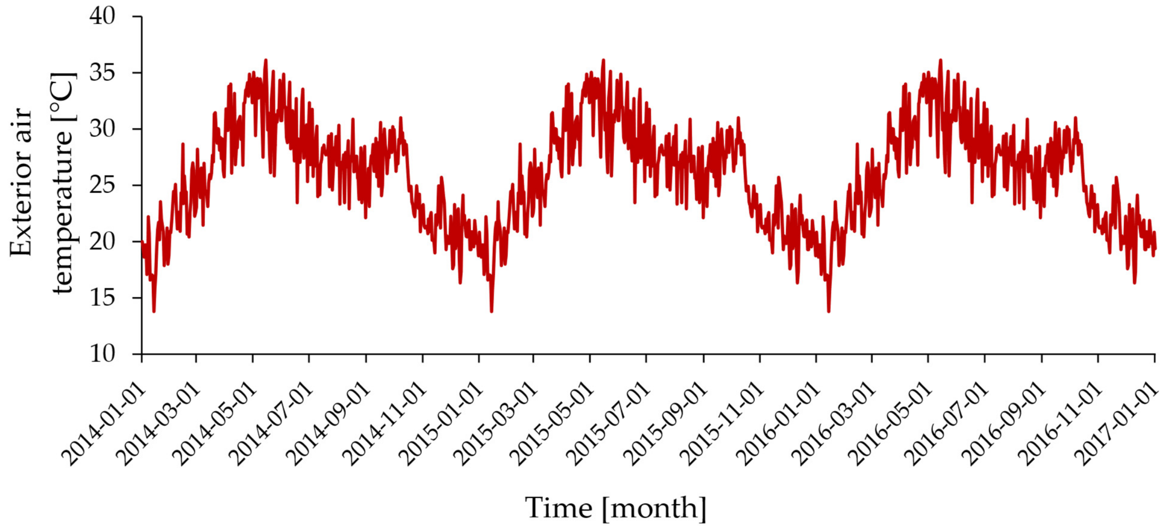

Figure 13. Variations in the exterior air temperature.

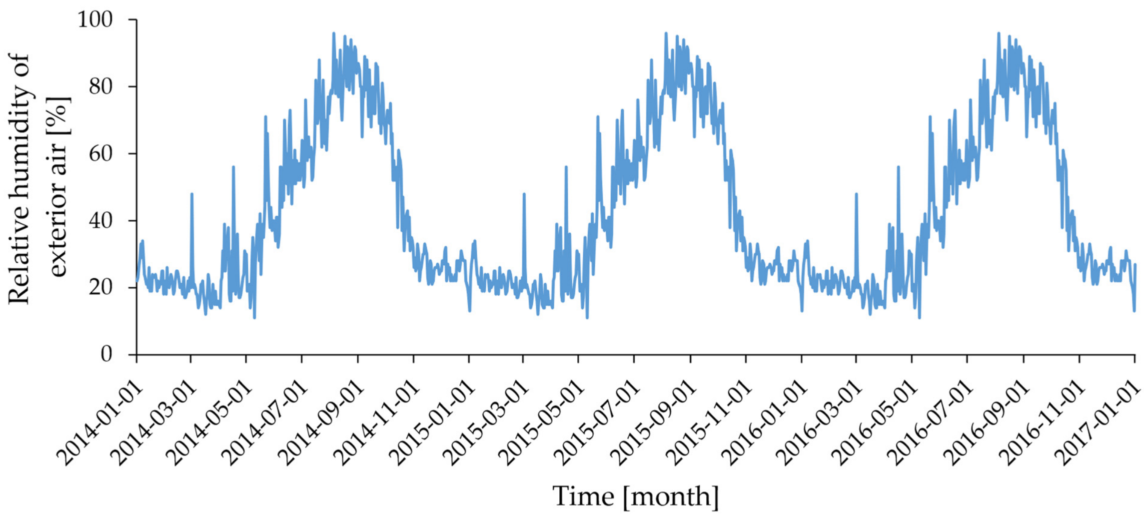

Figure 14. Variations in the relative humidity of exterior air.

Table 8. Summary of temperature variation in materials.

Case of Simulated Wall	Fraction of Incident Solar Radiation (%)	Exterior Wall Surface Temperature [°C]	Temperature in the Middle of the Wall [°C]	Interior Wall Surface Temperature [°C]
Cement block wall	1	15 to 35	18 to 31	20 to 29
	5	15 to 37	19 to 31	20 to 29
Earth brick wall	1	13 to 37	20 to 30	21 to 27
	5	13 to 38	20 to 30	22 to 27
Hemp concrete wall	1	9 to 45	18 to 31	22 to 24.5
	5	9 to 49	19 to 31	22 to 24.5

After the simulation of the walls, the difference in temperature of the main materials is visible. The interior temperature of the hemp concrete wall throughout the simulation hovers between 22 °C and 24.6 °C, with the exterior surface temperatures ranging from 10.8 °C to 32.8 °C for a maximum exterior air temperature of 43 °C and a minimum of 15 °C, respectively. The maximum interior temperature for cement block and earth brick walls are 28.7 °C and 27.0 °C, respectively. The observed temperature difference may be due to the hemp concrete's low thermal conductivity (λ) of 0.085 W/m·K, which is significantly lower than those of compressed earth brick (λ = 0.24 W/m·K) and cement block (λ = 1.2 W/m·K) walls, enabling the hemp concrete wall to efficiently regulate interior temperature. Figures 15 and 16 show the variation in the exterior and interior surface temperatures of the three wall assemblies studied.

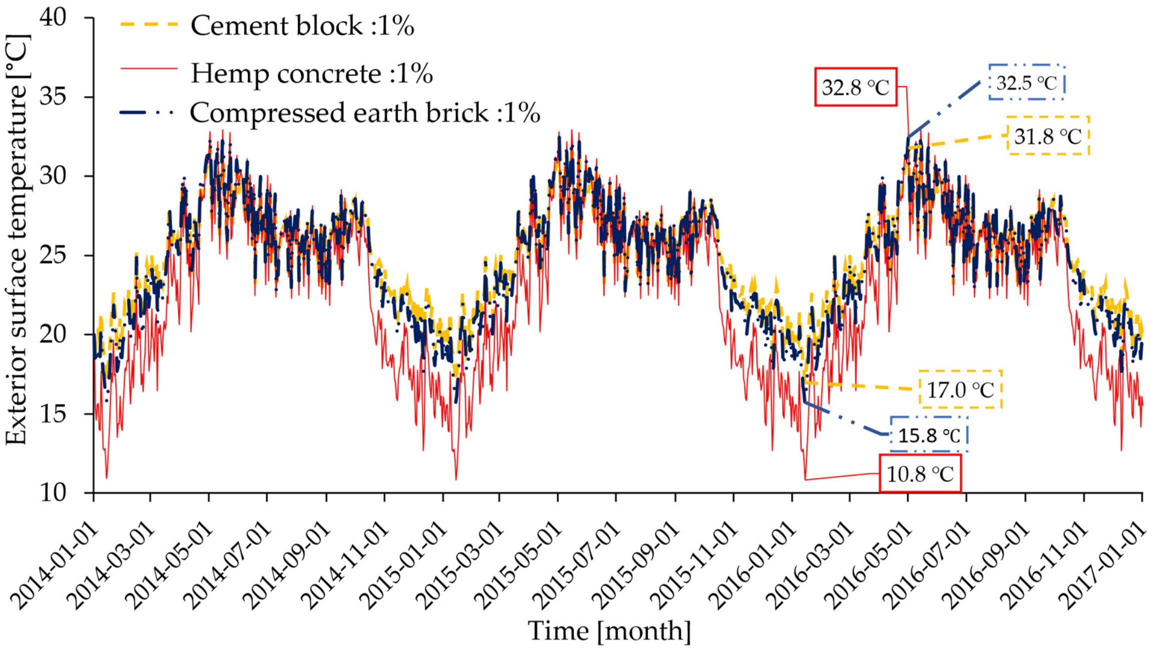

Figure 15. Variation in the exterior surface temperature of the main materials for an addition of 1% of solar incident radiation for three-year simulations.

The maximum absorption temperature by the exterior surface of the walls in summer was 32.8 °C for hempcrete walls, 31.8 °C for cement block walls, and 31.5 °C for compressed earth brick walls (Figure 15). In winter, the lowest temperature was observed for the hempcrete wall with a value of 10.8 °C. The fact that the exterior surface temperature of hempcrete walls is low helps limit heat loss, thus assisting in maintaining a comfortable and constant interior temperature [51]. The 43 °C highlighted in the corner of Figure 16 represents the peak exterior temperature recorded on a typical day in mid-May 2016, specifically at 1:00 PM. However, even at this high exterior temperature, the interior surface temperature of the hemp concrete wall remained comfortably below 25 °C, as shown in Figures 16 and 17c. In contrast, the interior surface temperatures of the compressed earth brick and cement block walls were significantly higher, reaching 27 °C and 29 °C, respectively, as shown in Figure 17a,b.

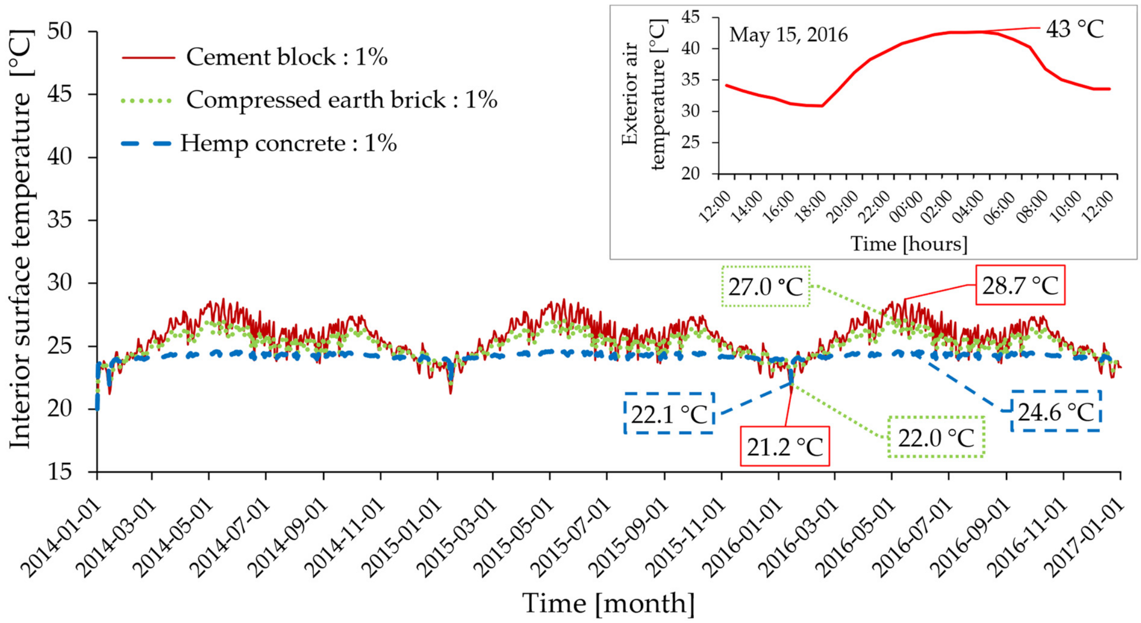

Figure 16. Variation in the interior surface temperature of the main materials for an addition of 1% of solar radiation incident for three years of simulation.

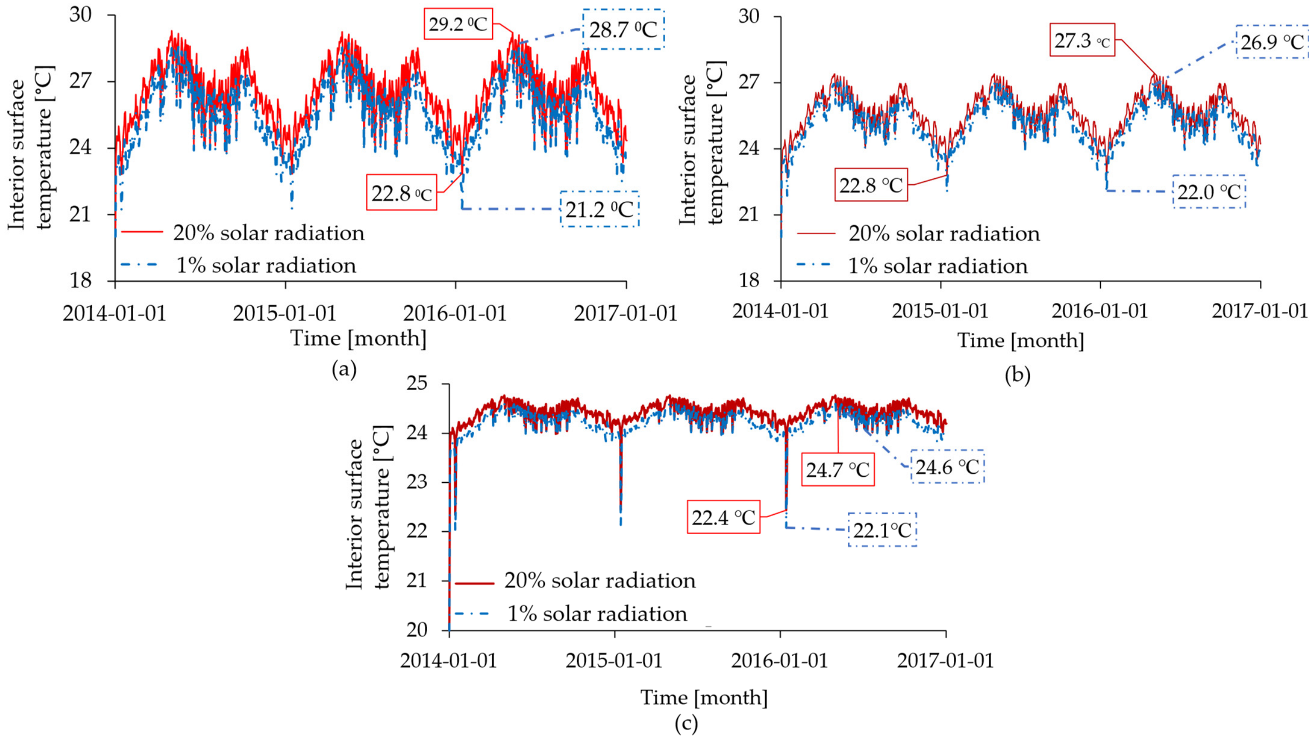

Figure 17. Temperature of the interior surface of the (**a**) cement block wall, (**b**) compressed earth brick, and (**c**) hemp concrete.

Hemp concrete stands out for its excellent ability to regulate the interior temperature of buildings, maintaining a stable and comfortable interior environment even under extreme exterior conditions. These findings are consistent with those of Bayol's experimental study and the numerical simulation results obtained by Asli et al. 2021 [20,52]. Other studies have also highlighted hemp concrete's advantageous thermal behavior and insulating properties [47,53]. Its low thermal conductivity contributes to its high thermal inertia, allowing it to absorb heat without a significant increase in interior temperature. Experimental characterizations of the thermal and moisture properties of hemp concrete have been studied by Bennaï et al. 2017 [54], showing that hemp can enhance the hygrothermal performance of buildings. This material effectively manages heat and humidity, improving comfort levels in buildings.

In scenarios with 20% solar radiation, the maximum interior temperature only increased by 0.12 °C for hemp concrete walls. In contrast, compressed earth brick walls saw an increase of 0.45 °C, and cement block walls showed an increase of 0.50 °C (Figure 17). These results highlight the thermal inertia of hemp concrete and its ability to gradually absorb and release heat, thereby preventing abrupt interior temperature changes in buildings. This quality makes hemp concrete an ideal material for constructing energy-efficient buildings that offer a stable interior environment, improve occupant comfort, and reduce the need for air conditioning systems in hot climates.

4. Discussion

The annual temperature variation amplitudes are higher for the cement block wall followed by the compressed earth brick wall. The hemp concrete walls tend to accumulate heat on their exterior surface while their interior surface temperature is between 22 and 25 °C regardless of the solar radiation exerted on their exterior surface (Figures 15, 16 and 17c). These temperatures are within the thermal comfort range for high-temperature countries, according to Meyer [55].

After this study, it should be noted that other materials may have similar hygrothermal properties to hemp concrete and could be used for building envelope design in hot climates. Such materials include those reinforced with straw, flax, wood, and yucca fibers. A study was conducted on the cob, a material made with clay and wheat fibers, which demonstrated promising hygrothermal properties [56]. Indeed, the aim of this study is to valorize the use of hemp concrete as a building material in hot climates. This study also aims to understand the thermal behavior of hemp concrete when it is integrated into the building envelope and to highlight the importance of integrating existing biobased materials into current construction in countries with high temperatures.

More authors have highlighted the renewed interest in the use of construction materials with low environmental impact in their work. However, in the field of construction, most of Africa uses cement, a material whose production emits 5% to 8% of greenhouse gases into the atmosphere [57]. Wood-frame houses with hemp concrete are economical in terms of energy demand for air-conditioning or heating as they are very good temperature and humidity regulators and an excellent acoustic damper according to the results obtained and to Tomovska [58]. With the 20% surplus of solar radiation exerted on the surface of a concrete wall, the external surface that receives this solar radiation varies from 41.4 °C to 61.4 °C [59], giving an internal temperature variation from 22 to 25 °C for a hemp concrete wall in this study. Experimental studies by Costantine et al. showed that for exterior temperatures between 12 and 43 °C, interior temperatures varied between 22 and 26 °C. These results are consistent with those of the present numerical study [60]. In addition, hemp concrete can be used in low-temperature countries, if the wall is well insulated and there is no water infiltration [61]. Referring to Figure 9, in addition to being an environmentally friendly, energy-efficient building material, it is suitable for typical construction in Africa. The addition of hemp concrete in African construction could be another very interesting alternative material among the local materials of Africa or other high-temperature countries.

5. Conclusions

The selection of materials is crucial to ensure optimal performance of the building envelope. The simulations have revealed that the interior temperatures of wall assemblies made of cement blocks and compressed earth bricks vary depending on the external climate, while those of hemp concrete remain stable in cases 1% and 5% fractions. Particularly, the high interior temperatures of cement block walls and compressed earth brick walls require additional air conditioning, as their interior temperature exceeds the comfort temperature of 4.5 °C and 2.6 °C, respectively. Regarding specific materials:

- Cement block walls and compressed earth brick walls display maximum interior temperatures of 29.2 °C and 27.3 °C, respectively, surpassing the set temperature of 24 °C, necessitating the use of air conditioning.
- Hemp concrete stands out for its low thermal conductivity (0.085 W/mK), enabling effective control of interior temperature. Simulations indicate variations in interior temperature between 22 °C and 24.6 °C, thereby avoiding the need for air conditioning.
- The hemp concrete wall accumulates more heat on its exterior surface in summer than the other walls, with significant temperature variations between winter and summer. The application of incident solar radiation fractions of 1% and 5% resulted in similar interior temperatures, indicating that the 5% increase in overall solar radiation did not affect the interior temperature of the walls but that of the exterior surface.
- Additionally, with 20% of solar radiation, hemp concrete walls experience only a slight increase of 0.12 °C in maximum interior temperature, while compressed earth brick walls and cement block walls show respective increases of 0.45 °C and 0.50 °C.

For a more comprehensive study, an experimental investigation comparing the hygrothermal performance of hemp concrete to numerical simulations would be beneficial. This would further explore the potential of hemp concrete as a sustainable and eco-friendly building material. It would also be important to include simulations with weather data encompassing high temperatures and humidity levels, as well as an increased risk of condensation to assess its ability to dissipate accumulated moisture within the wall assembly.

Author Contributions: Conceptualization, A.K., W.M. and C.M.O.-P.; data curation, A.K., W.M. and C.M.O.-P.; formal analysis, A.K.; investigation, A.K. and W.M.; methodology, A.K., W.M. and C.M.O.-P.; project administration, W.M. and C.M.O.-P.; resources, W.M. and C.M.O.-P.; software, A.K.; supervision, W.M. and C.M.O.-P.; validation, W.M. and C.M.O.-P.; visualization, A.K.; writing—original draft preparation, A.K.; writing—review and editing, W.M. and C.M.O.-P. All authors have read and agreed to the published version of the manuscript.

Funding: This research was funded by the Programme Canadien de Bourse de la Francophonie (PCBF).

Data Availability Statement: The original contributions presented in the study are included in the article, further inquiries can be directed to the corresponding author.

Acknowledgments: The authors thank Dhakal, Ujwal and Lamalle, Marie for providing the data to validate the WUFI software before its use for hygrothermal simulation.

Conflicts of Interest: The authors declare no conflicts of interest.

References

1. Thibault, H.; El Habib, E.A.; L'efficacité énergétique dans le bâtiment en Méditerranée. Futuribles 2011, 376, 47–59. Available online: http://planbleu.org/sites/default/files/publications/2-3-fr_futuribles_2011_376_ee.pdf (accessed on 1 March 2023).
2. Bakkour, A.; Ouldboukhitine, S.-E.; Biwole, P.; Amziane, S. A review of multi-scale hygrothermal characteristics of plant-based building materials. *Constr. Build. Mater.* **2024**, *412*, 134850. [CrossRef]
3. Commission de Coopération Environnementale. *Le Bâtiment Écologique en Amérique du Nord: Débouchés et Défis*; Commission de Coopération Environnementale: Montreal, QC, Canada, 2013; p. 80.
4. William, M.A.; Suárez-López, M.J.; Soutullo, S.; Hanafy, A.A. Building envelopes toward energy-efficient buildings: A balanced multi-approach decision making. *Int. J. Energy Res.* **2021**, *45*, 21096–21113. [CrossRef]
5. Scheifel, G.; Bill, W.J.; Kemptville. La Culture du Chanvre Industriel. 2000. Available online: http://www.omafra.gov.on.ca/french/crops/facts/00-068.htm (accessed on 13 February 2023).
6. Berger, J.; Contribution à la Modélisation Hygrothermique des Bâtiments: Application des Méthodes de Réduction de Modèle. Grenoble. 2014, p. 225. Available online: https://theses.hal.science/tel-01127189 (accessed on 13 February 2023).
7. ONUDC. Nations Unies, Office Contre la Drogue et le Crime: Le Cannabis en Afrique. 2007. 22p. Available online: www.unodc.org (accessed on 13 February 2023).

8. Chamoin, J. Optimisation des Propriétés (Physiques, Mécaniques et Hydriques) de Bétons de Chanvre par la Maîtrise de la Formulation. INSA de Rennes: Rennes, France. 2013. Available online: https://theses.hal.science/tel-00934732 (accessed on 13 February 2023).
9. Motamedi, S.; Rousse, D.R.; Promis, G. The evolution of crop-based materials in the built environment: A review of the applications, performance, and challenges. *Energies* **2023**, *16*, 5252. [CrossRef]
10. Fortin, P. *Formulation d'un Liant Pouzzolanique Pour la Confection d'un Béton Végétal Hygroscopique*; École de Technologie Supérieure: Montreal, QC, Canada, 2022. Available online: https://espace.etsmtl.ca/id/eprint/3095/ (accessed on 19 March 2024).
11. Niyigena, C.S.; Variabilité des Performances de Bétons de Chanvre en Fonction des Caractéristiques de la Chènevotte Produite en Auvergne. In Université Blaise Pascal-Clermont-Ferrand II. 2016. Available online: https://theses.hal.science/tel-01487057 (accessed on 25 September 2023).
12. Shea, A.; Lawrence, M.; Walker, P. Hygrothermal performance of an experimental hemp–lime building. *Constr. Build. Mater.* **2012**, *36*, 270–275. [CrossRef]
13. ANSI/ASHRAE. *Criteria for Moisture-Control Design Analysis in Buildings*; ASHRAE: Atlanta, GA, USA, 2016. Available online: https://www.techstreet.com/standards/ashrae-160-2016?product_id=1939166 (accessed on 25 September 2023).
14. Łapka, P.; Brzyski, P.; Pietrak, K.; Cieślikiewicz, Ł.; Suchorab, Z. Hygro-thermal characterization of the hemp concrete modified with the gum Arabic admixture. *Constr. Build. Mater.* **2023**, *368*, 130392. [CrossRef]
15. Rahim, M.; Douzane, O.; Le, A.T.; Promis, G.; Langlet, T. Characterization and comparison of hygric properties of rape straw concrete and hemp concrete. *Constr. Build. Mater.* **2016**, *102*, 679–687. [CrossRef]
16. Samri, D. *Analyse Physique et Caractérisation Hygrothermique des Matériaux de Construction: Approche Expérimentale et Modélisation Numérique*; Ecole Nationale des Travaux Publics de l'Etat: Vaulx-en-Velin, France, 2008. Available online: https://theses.insa-lyon.fr/publication/2008ISAL0067/these.pdf (accessed on 27 September 2023).
17. Collet, F.; Pretot, S. Thermal conductivity of hemp concretes: Variation with formulation, density and water content. *Constr. Build. Mater.* **2014**, *65*, 612–619. [CrossRef]
18. Martínez, B.; Mendizabal, V.; Roncero, M.B.; Bernat-Maso, E.; Gil, L. Towards sustainable building solutions: Development of hemp shiv-based green insulation material. *Constr. Build. Mater.* **2024**, *414*, 134987. [CrossRef]
19. Latif, E. Experimental analysis of moisture-dependent thermal conductivity, and hygric properties of novel hemp–shive insulations with numerical assessment of their in-built hygrothermal and energy performance. *Materials* **2024**, *17*, 486. [CrossRef]
20. Bayol, D. Eco-Construction-Bioclimatique-le Beton de Chanvre Vous Permet un Bonus Pour Construire Plus. 2016. Available online: http://db-chanvre.com/la-construction-passive/ (accessed on 27 September 2023).
21. Gauthier, G. Art Can-Construction en Chanvre. 2018. Available online: https://maisonenchanvre.com/avantages-du-chanvre (accessed on 27 September 2023).
22. Cieski, J. Materiaux Biosourcés, Comportement Hygrothermique d'une Paroi en Beton de Chanvre. Available online: https://seminairemateriaux.files.wordpress.com/2014/06/r9-mc3a9moire.pdf (accessed on 25 April 2023).
23. Youssef, A.; Prise en Compte des Apports Mécaniques du Béton de Chanvre Pour le Calcul de Structure Bois/Béton de Chanvre et Métal/Béton de Chanvre. Lorient. 2017. Available online: https://theses.hal.science/tel-01535694 (accessed on 25 April 2023).
24. Rahim, M.; Douzane, O.; Le, A.T.; Promis, G.; Laidoudi, B.; Crigny, A.; Dupre, B.; Langlet, T. Characterization of flax lime and hemp lime concretes: Hygric properties and moisture buffer capacity. *Energy Build.* **2015**, *88*, 91–99. [CrossRef]
25. Mazhoud, B.; Collet, F.; Prétot, S.; Lanos, C. Effect of hemp content and clay stabilization on hygric and thermal properties of hemp-clay composites. *Constr. Build. Mater.* **2021**, *300*, 123878. [CrossRef]
26. Pochwała, S.; Makiola, D.; Anweiler, S.; Böhm, M. The heat conductivity properties of hemp–lime composite material used in single-family buildings. *Materials* **2020**, *13*, 1011. [CrossRef] [PubMed]
27. Benmahiddine, F.; Bennai, F.; Charaka, A.; Hamami, A.E.A.; Tahakourt, A.; Belarbi, R. Multi-scale analysis of the effects of hysteresis on the hydrothermal behaviour of bio-based materials: Application to hemp concrete. *Constr. Build. Mater.* **2024**, *411*, 134107. [CrossRef]
28. Boisyvon, A. Comparatif des Performances Envrionnementales du Béton et du Béton de Chanvre-Etude du Cas de Deux batiments D'habitation Construits par Val Touraine Habitat à Nouzilly (37). 2015. 8p. Available online: www.cerema.fr (accessed on 2 April 2023).
29. Künzel, H.M.; Germany, F.I. Modeling Air Leakage in Hygrothermal Envelope Simulation. In Proceedings of the BEST 3 Conference, Atlanta, GA, USA, 2–4 April 2012; p. 26.
30. Dhakal, U.; Berardi, U.; Gorgolewski, M.; Richman, R. Hygrothermal performance of hempcrete for Ontario (Canada) buildings. *J. Clean. Prod.* **2017**, *142*, 3655–3664. [CrossRef]
31. Muhit, I.B.; Omairey, E.L.; Pashakolaie, V.G. A holistic sustainability overview of hemp as building and highway construction materials. *Build. Environ.* **2024**, *256*, 11470. [CrossRef]
32. Wyss, U.; La Construction en" Matériaux locaux": État d'un Secteur à Potentiel Multiple; Suisse. Direction du Développement et de la Coopération. 2005. Available online: https://jaga.afrique-gouvernance.net/_docs/resource_fr_65911.pdf (accessed on 20 October 2022).
33. İlcan, H.; Özkılıç, H.; Tuğluca, M.S.; Şahmaran, M. Interlayer mechanical performance of 3D-printed cementitious systems: A comprehensive study on operational and material parameters. *Constr. Build. Mater.* **2024**, *419*, 135463. [CrossRef]

34. Wang, X.; Li, W.; Guo, Y.; Kashani, A.; Wang, K.; Ferrara, L.; Agudelo, I. Concrete 3D printing technology in sustainable construction: A review on raw materials, concrete types and performances. *Dev. Built Environ.* **2024**, *17*, 100378. [CrossRef]
35. Li, H.; Addai-Nimoh, A.; Kreiger, E.; Khayat, K.H. Methodology to design eco-friendly fiber-reinforced concrete for 3D printing. *Cem. Concr. Compos.* **2024**, *147*, 105415. [CrossRef]
36. Gamage, K.; Fawzia, S.; Zahra, T.; Teixeira, M.B.F.; Ramli Sulong, N.H. Advancement in Sustainable 3D Concrete Printing: A Review on Materials, Challenges, and Current Progress in Australia. *Buildings* **2024**, *14*, 494. [CrossRef]
37. Hosseinzadehfard, E.; Mobaraki, B. Investigating concrete durability: The impact of natural pozzolan as a partial substitute for microsilica in concrete mixtures. *Constr. Build. Mater.* **2024**, *419*, 135491. [CrossRef]
38. Guangyao, D.; Songmin, L.; Xiaoling, W.; Yazhi, Z.; Qihang, W. Optimal Design of Ecological Concrete Mix Proportion Based on AHP-GWO-BP Neural Network. *Int. J. Environ. Res.* **2024**, *18*, 24. [CrossRef]
39. Mobaraki, B.; Pascual, F.J.C.; Lozano-Galant, F.; Soriano, R.P.; Lozano-Galant, J.A. Characterization of the thermal transmittance in buildings using low-cost temperature sensors. In Proceedings of the International Conference on Building Energy and Environment, Virtual, 25–29 July 2022; pp. 403–412. [CrossRef]
40. Mobaraki, B.; Komarizadehasl, S.; Castilla Pascual, F.J.; Lozano-Galant, J.A.; Porras Soriano, R. A novel data acquisition system for obtaining thermal parameters of building envelopes. *Buildings* **2022**, *12*, 670. [CrossRef]
41. Bennai, F.; Ferroukhi, M.Y.; Benmahiddine, F.; Belarbi, R.; Nouviaire, A. Assessment of hygrothermal performance of hemp concrete compared to conventional building materials at overall building scale. *Constr. Build. Mater.* **2022**, *316*, 126007. [CrossRef]
42. Sawadogo, M.; Benmahiddine, F.; Godin, A.; Duquesne, M.; Belarbi, R.; Hamami, A. Development and hygrothermal performance analysis of a novel eco-friendly insulating wall under various climatic conditions. *Build. Environ.* **2023**, *245*, 110841. [CrossRef]
43. Birjukovs, M.; Sinka, M.; Jakovics, A.; Bajare, D. Combined in situ and in silico validation of a material model for hempcrete. *Constr. Build. Mater.* **2022**, *321*, 126051. [CrossRef]
44. Jirgensone, B.; Birjukovs, M.; Sinka, M.; Jakovics, A.; Bajare, D. Hygrothermal performance of hempcrete in a multi-layer wall envelope. *J. Build. Eng.* **2024**, *84*, 108359. [CrossRef]
45. Benkhaled, M.; Ouldboukhitine, S.-E.; Bakkour, A.; Amziane, S. Sensitivity analysis of the parameters for assessing a hygrothermal transfer model HAM in bio-based hemp concrete material. *Int. Commun. Heat Mass Transf.* **2022**, *132*, 105884. [CrossRef]
46. Yadav, M.; Saini, A. Opportunities & challenges of hempcrete as a building material for construction: An overview. *Mater. Today Proc.* **2022**, *65*, 2021–2028. [CrossRef]
47. Barbhuiya, S.; Das, B.B. A comprehensive review on the use of hemp in concrete. *Constr. Build. Mater.* **2022**, *341*, 127857. [CrossRef]
48. Lamalle, M. Bloc de Béton de bois, Une alternative au Bloc traditionnel?-Étude des Caractéristiques Mécaniques, Thermiques et Écologiques d'un Bloc de Coffrage en Béton de Bois. In *Faculté des Sciences Appliquées*; Université de Liége: Liège, Belgium, 2016; p. 172. Available online: http://hdl.handle.net/2268.2/1283 (accessed on 2 January 2022).
49. *EN15026*; Hygrothermal performance of building components and building elements - Assessment of moisture transfer by numerical simulation. European Committee for Standardization (CEN): Brussels, Belgium, 2007.
50. *ANSI/ASHRAE 160*; Criteria for Moisture-Control Design Analysis in Buildings. ASHRAE: Atlanta, GA, USA, 2009. Available online: https://www.ashrae.org/file%20library/technical%20resources/standards%20and%20guidelines/standards%20addenda/160_2009_e_201601209.pdf (accessed on 3 April 2022).
51. Haik, R.; Peled, A.; Meir, I. The thermal performance of lime hemp concrete (LHC) with alternative binders. *Energy Build.* **2020**, *210*, 109740. [CrossRef]
52. Asli, M.; Brachelet, F.; Sassine, E.; Antczak, E. Thermal and hygroscopic study of hemp concrete in real ambient conditions. *J. Build. Eng.* **2021**, *44*, 102612. [CrossRef]
53. Hachem, C.E.; Moussa, J.; Abahri, K. Thermal Study of Hemp Concrete Behavior when Subjected to High Temperatures by X-ray Microtomography. In Proceedings of the International RILEM Conference on Synergising Expertise towards Sustainability and Robustness of CBMs and Concrete Structures, Milos, Greece, 14–16 June 2023; pp. 1318–1329.
54. Bennai, F.; Issaadi, N.; Abahri, K.; Belarbi, R.; Tahakourt, A. Experimental characterization of thermal and hygric properties of hemp concrete with consideration of the material age evolution. *Heat Mass Transf.* **2018**, *54*, 1189–1197. [CrossRef]
55. Makaka, G.; Meyer, E. Temperature stability of traditional and low-cost modern housing in the Eastern Cape, South Africa. *J. Build. Phys.* **2006**, *30*, 71–86. [CrossRef]
56. Ouellet-Plamondon, C.; Kaboré, A. *Hygrothermal Measurement of Heavy Cob Materials*; Springer Nature: Cham, Switzerland, 2023; pp. 1243–1252. [CrossRef]
57. Le Quéré, C.; Peters, G.P.; Andres, R.J.; Andrew, R.M.; Boden, T.A.; Ciais, P.; Friedlingstein, P.; Houghton, R.A.; Marland, G.; Moriarty, R. Global carbon budget 2013. *Earth Syst. Sci. Data* **2014**, *6*, 235–263. [CrossRef]
58. Tomovska, R.; Radivojević, A. Tracing sustainable design strategies in the example of the traditional Ohrid house. *J. Clean. Prod.* **2017**, *147*, 10–24. [CrossRef]
59. Boyer, D.; Sur L'augmentation de L'albédo des Toitures de Batiments Pour Diminuer la Progressiobs des Changements Climatiques. Supérieures GCH-Proj. D'études 2010, p. 34. Available online: https://www.ecohabitation.com/media/archives/files/Projet%20pour%20combattre%20les%20changements%20climatiques.pdf (accessed on 9 December 2023).

60. Costantine, G.; Maalouf, C.; Moussa, T.; Polidori, G. Experimental and numerical investigations of thermal performance of a Hemp Lime external building insulation. *Build. Environ.* **2018**, *131*, 140–153. [CrossRef]
61. Kabore, A.; Maref, W.; Plamondon, C. Hygrothermal performance of the building envelope with low environmental impact: Case of a hemp concrete envelope. In Proceedings of the 8th International Building Physics Conference (IBPC 2021), Copenhagen, Denmark, 25–27 August 2021.